



## Robust Controller for a Grid-Connected Photovoltaic Semi Quasi Inverter System

**K. O. Lawal\*, A. S. Adamu, G. Olarinoye, I. Abdulwahab**

Ahmadu Bello University Zaria, Kaduna State, Nigeria

\*[engralook@gmail.com](mailto:engralook@gmail.com)

Research Article

### Abstract

This work present semi quasi source inverter (SQSI) that operate on two active state without the application of shoot through mode. An  $H_\infty$  (H infinity) controller was developed using a generalized plant obtained from SQSI for PV grid connected system. The SQSI reduces the stresses on circuit component, provides ample and also limit the start-up in rush current for power quality and reliability. Asalp swarm-based Maximum Power Point Tracking (MPPT) algorithm was used to track the maximum power from the PV(photovoltaic) and closed loop system was obtained to monitor the entire network. The simulation results obtained from MATLAB/Simulink environment guaranteed the system performance. The results obtained were compared with the results obtained when quasi- admittance source inverter (QYSI) were used. The Fast Fourier Transform (FFT) analysis showed that the THD was reduced from 0.67% to 0.61%. This shows that the SQSI is a transformerless kind of inverter and outperformed the THD value obtained from the QYSI a transformer based. Due to low level of harmonics in the current waveform. The tracking efficiency of the system also improve from 97.1% to 99.68% using the salp swarm algorithm. The frequency deviation as result of sudden load variation was monitored which kept the output voltage and current almost in phase with an improve power factor from 0.90 to 0.96 as compared to robust controller for grid connected quasi admittance source inverter (QYSI) for PV system.

doi: [10.5455/nje.2023.30.03.08](https://doi.org/10.5455/nje.2023.30.03.08)

Copyright © Faculty of Engineering, Ahmadu Bello University, Zaria, Nigeria.

### Keywords

Semi Quasi Source Inverter; H Infinity Controller; Fast Fourier Transform; Harmonics and Frequency

### Article History

Received: – July, 2023

Reviewed: – September, 2023

Accepted: – October, 2023

Published: –December, 2023

### 1.0 Introduction

The need for uninterrupted supply of energy made renewable energy (RE) prevail above the conventional mode of generating energy (Babaita *et al.*, 2022; Iliyasu *et al.*, 2022). The increase in the demand for supply gives way to RE such as solar, wind and fuel cell energy and so on gainmore access in the power network (Abdulwahab *et al.*, 2022; Hassan 2017). Output of the photovoltaic source produces a DC voltage, hence an inverter is needed to be used as an intermediary between the solar panel and the grid connected AC voltage (Deepamangai & Manoharan 2019). However, there is need to provide an inverter other than traditional voltage source inverter that will accommodate the buck and boost stage without the use of DC-DC converter and also for protecting system against the DC current injection and minimization of connection effect from the impact of DC side and the load(Santhoshi *et al.*, 2019; Venkatesan *et al.*, 2019). The impedance source inverter (ZSI)source inverter is the combination of a DC-DC boost converter system with a voltage source inverter without using any additional power electronics (Deepamangai & Manoharan 2019). The important of inductor in quasi impedance source inverter (QZSI) network will limit the current ripple in the devices while boosting

but the shoot through state could not be eliminated (Fang *et al.*, 2018; Rasool *et al.*, 2019).

The semi quasi-inverter is used mostly with a renewable-energy in photovoltaic system for distributed generation, it obtained from the modification of impedance inverter which contain LC network. The distinguish feature of the Z-source inverter is the shoot-through state use for boosting stage of the Z-source system which is not used in semi-quasi source inverter (SQSI). Therefore, the operation principle of this inverter is quite different (Ismeil *et al.*, 2018).A semi quasi-inverter designed with some passive components such as coupled inductor and capacitor. The SQSI has two active switches producing sinusoidal voltage and placed at the AC side in order to eliminate shoot through state of the quasi-type inverter. The AC voltage output and the input DC source of the SQSI have the same ground. As a result, the leakage ground current is reduced. This is a preferred characteristic for non-isolated grid-connected inverters, mostly in PV application. The photovoltaic panel extract maximum power from the renewable energy source and produce quality voltage AC output (Abdelrahem *et al.*, 2019).

In a PV system, in order to obtain adequate and effective DC-AC conversion, impedance source inverter (ZSI) is a remarkable option. A ZSI is a combination of inductor and capacitor. It has the ability of buck and boost, that is, it

exhibits the primary function of voltage and current source inverter. Different modification are frequently adopted on the ZSI system topology in order to improve their topologies. However, more schemes that will improve the power quality still need to be developed. Ismeil *et al.*, (2018) presented a single phase cascaded SQSI for PV application with a nonlinear sinusoidal pulse width modulation (SPWM) technique. The technique was able to achieve appreciable result by placing independent maximum power point tracking device on each cell within the module for both conditions (total and partial shading). This therefore, increases the complexity of the system. Deepamangai & Manoharan (2019) present an impedance source inverter topology which overcome the traditional voltage and current source inverter limitation. The impedance topology reduced the number of switches and improved the power stability of the system with adequate switching frequency. However, the proposed work could not account for the inductor leakage current.

Hence, this research has presented a SQSI for adequate system reliability. The aim of work is to develop an optimal control for the SQSI by developing H infinity controller for grid connected inverter that play a vital role in attenuating disturbances such as variation in impedance, voltage drop and harmonics from the system. The salp swarm algorithm on the other hand was implemented to track the Maximum Power Point from the PV array. This research work eliminate the stress on the inverter component and problem of shoot through state which hinder the reliability of larger inverter system by destroying the upper and lower switch on the same phase during shoot through mode (short circuit). The aforementioned limitations are the problems that this research seeks to address by introducing a semi quasi source inverter.

## 2.0 Methodology

The objectives of this research work were actualized through the following steps.

### 2.1 Semi Quasi Source Inverter Modelling

It consists of two states switches  $S_1$  and  $S_2$  which operate in complementary conduction mode (CCM). In CCM, the first complementary mode of the inverter  $S_1$  is ON and  $S_2$  OFF, with a duty ratio (D) achieved when capacitor  $C_1$  and the input voltage source charge the two inductors and the inductors currents increase. This state can be represented in matrix form, the state space equation becomes:

$$\dot{x} = B_q x + F_q v \quad (1)$$

$$\frac{df}{dt} \begin{bmatrix} i_{L1} \\ i_{L2} \\ v_{c1} \\ v_{c2} \end{bmatrix} = \begin{bmatrix} -\frac{R}{L_1} & 0 & \frac{1}{L_1} & 0 \\ 0 & -\frac{R}{L_2} & 0 & \frac{1}{L_2} \\ \frac{1}{C_1} & 0 & 0 & 0 \\ 0 & \frac{1}{C_2} & 0 & 0 \end{bmatrix} \begin{bmatrix} i_{L1} \\ i_{L2} \\ v_{c1} \\ v_{c2} \end{bmatrix} + \begin{bmatrix} -\frac{1}{L_1} & 0 \\ 0 & 0 \\ 0 & 0 \\ 0 & 0 \end{bmatrix} \begin{bmatrix} V_{in} \\ i_o \end{bmatrix} \quad (2)$$

Where

$\dot{x} = B_q x + F_q v$  denotes the state space equation

$$B_q = \begin{bmatrix} -\frac{R}{L_1} & 0 & 0 & \frac{1}{L_1} \\ 0 & -\frac{R}{L_2} & \frac{1}{L_2} & 0 \\ 0 & -\frac{1}{C_1} & 0 & 0 \\ -\frac{1}{C_2} & 0 & 0 & 0 \end{bmatrix}, F_q = \begin{bmatrix} \frac{1}{L_1} & 0 \\ 0 & 0 \\ 0 & 0 \\ 0 & 0 \end{bmatrix}, x = \begin{bmatrix} i_{L1} \\ i_{L2} \\ v_{c1} \\ v_{c2} \end{bmatrix}, v = \begin{bmatrix} V_{in} \\ i_o \end{bmatrix}$$

Where  $i_L$  denotes the inductor current,  $V_C$  depicts the capacitor voltage,  $i_o$  denotes the output current while  $V_{in}$  denotes input voltage.

The second mode of the active state II, the inverter  $S_1$  is OFF and  $S_2$  is ON, with a duty ratio of  $1 - D$  the two inductors become the source and the inductor current is decreased. The inductors current decreased by transferring energy through the capacitors to the connected load. The space equations of the above scenario is as follows:

$$\dot{x} = B_A x + F_A v \quad (3)$$

$$\begin{bmatrix} i_{L1} \\ i_{L2} \\ v_{c1} \\ v_{c2} \end{bmatrix} = \begin{bmatrix} -\frac{R}{L_1} & 0 & 0 & 0 \\ 0 & -\frac{R}{L_2} & 0 & 0 \\ 0 & -\frac{1}{C_1} & 0 & 0 \\ -\frac{1}{C_2} & 0 & 0 & 0 \end{bmatrix} \begin{bmatrix} i_{L1} \\ i_{L2} \\ v_{c1} \\ v_{c2} \end{bmatrix} + \begin{bmatrix} -\frac{1}{L_1} & 0 \\ 0 & 0 \\ 0 & \frac{1}{C_1} \\ 0 & \frac{1}{C_2} \end{bmatrix} \begin{bmatrix} V_{in} \\ i_o \end{bmatrix} \quad (4)$$

Where

$$A_s = \begin{bmatrix} -\frac{R}{L_1} & 0 & 0 & 0 \\ 0 & -\frac{R}{L_2} & 0 & 0 \\ 0 & -\frac{1}{C_1} & 0 & 0 \\ -\frac{1}{C_2} & 0 & 0 & 0 \end{bmatrix}, F_s = \begin{bmatrix} -\frac{1}{L_1} & 0 \\ 0 & 0 \\ 0 & \frac{1}{C_1} \\ 0 & \frac{1}{C_2} \end{bmatrix}, x = \begin{bmatrix} i_{L1} \\ i_{L2} \\ v_{c1} \\ v_{c2} \end{bmatrix}, v = \begin{bmatrix} V_{in} \\ i_o \end{bmatrix}$$

During a complete oscillation, the two active states are donated with  $D$  and  $1 - D$ . The overall state space equation for one switching state can be derived as follow

$$\dot{x} = (B_q x + F_q v).D + (B_A x + F_A v).(1 - D) \quad (5)$$

The derived space equation is therefore expressed as shown in equation (6)

$$\frac{df}{dt} \begin{bmatrix} i_{L1} \\ i_{L2} \\ v_{c1} \\ v_{c2} \end{bmatrix} = \begin{bmatrix} -\frac{R}{L_1} & 0 & \frac{1-D}{L_1} & 0 \\ 0 & -\frac{R}{L_2} & 0 & \frac{1-D}{L_2} \\ \frac{1-D}{C_1} & -\frac{D}{C_1} & 0 & 0 \\ -\frac{D}{C_2} & \frac{1-D}{C_2} & 0 & 0 \end{bmatrix} \begin{bmatrix} i_{L1} \\ i_{L2} \\ v_{c1} \\ v_{c2} \end{bmatrix} + \begin{bmatrix} \frac{1-2D}{L_1} & 0 \\ 0 & 0 \\ 0 & \frac{D}{C_1} \\ 0 & \frac{D}{C_2} \end{bmatrix} \begin{bmatrix} V_{in} \\ i_o \end{bmatrix} \quad (6)$$

Since the value of inductance  $L_1$  and  $L_2$  equal  $L$  and the capacitance value  $C_1$  and  $C_2$  equal  $C$

Hence

$$\tilde{i}_L = \tilde{i}_{L1} = \tilde{i}_{L2} \quad (7)$$

$$\tilde{V}_C = \tilde{V}_{C1} = \tilde{V}_{C2} \quad (8)$$

The system is reduced as

$$\frac{df}{dt} \begin{bmatrix} \tilde{i}_L \\ \tilde{V}_C \end{bmatrix} = \begin{bmatrix} -\frac{R}{L} & \frac{1-D}{L} \\ \frac{1-D}{L} & 0 \end{bmatrix} \begin{bmatrix} \tilde{i}_L \\ \tilde{V}_C \end{bmatrix} + \begin{bmatrix} \frac{1-2D}{L} & 0 \\ 0 & \frac{D}{C_1} \end{bmatrix} \begin{bmatrix} V_{in} \\ i_o \end{bmatrix} \quad (9)$$

Where

$$A = \begin{bmatrix} -\frac{R}{L} & \frac{1-D}{L} \\ \frac{1-D}{L} & 0 \end{bmatrix}, F = \begin{bmatrix} \frac{1-2D}{L} & 0 \\ 0 & \frac{D}{C_1} \end{bmatrix}, x = \begin{bmatrix} \tilde{i}_L \\ \tilde{V}_C \end{bmatrix}, v = \begin{bmatrix} V_{in} \\ i_o \end{bmatrix}$$

The value of  $V_C$  and  $i_L$  becomes

Where  $V_c = V_0$  (10)

$i_{L2} = i_0$  (11)

From the above equation the steady state system for the proposed semi quasi (inverter) inductor voltage and capacitor current can be written thus

$$V_0 = \frac{1-2D}{1-D} V_{in} \quad (12)$$

$$I_0 = \frac{1-D}{D} I_i \quad (13)$$

Where

$$D = \frac{t_{on}}{T} \text{ Duty ratio of switch } S_1$$

The sinusoidal output of the inverter can be given in equation (14)

$$V_0 = V \sin(\omega t) \quad (14)$$

The modulation index can be written as

$$M = \frac{V}{V_{in}} \quad (15)$$

Substitute equation (14) and (15) into equation (12)

$$D = \frac{1 - M \sin(\omega t)}{2 - M \sin(\omega t)} \quad (16)$$

The duty ratio D obtained from the equation above is used as the reference signal for firing the switches of the semi quasi-inverter as obtained from H infinity controller

## 2.2 Design of the Controller

The  $H_\infty$  controller was used to achieve better power reliability and voltage stability. It also enhance the reduction of total harmonic distortion (THD) while tracking the references point, for sudden changes in load and grid impedance. Figure 1 illustrates the configuration system of the  $H_\infty$  controller.

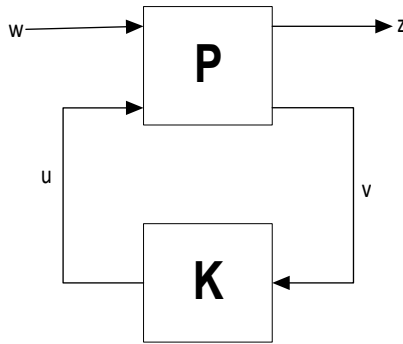


Figure 1: H Infinity Configuration

Objective function of the system is stated defined in equation (17)

$$\|F_l(P, K)\|_\infty \cong \max \bar{\sigma}(F_l(P, K)(j\omega)) \quad (17)$$

$$\frac{z}{y} = \begin{bmatrix} P_{11}(s) & P_{12}(s) \\ P_{21}(s) & P_{22}(s) \end{bmatrix} \cdot \begin{bmatrix} w \\ u \end{bmatrix} \quad (18)$$

Where u depicts the systems control input. y represents the measured output for H infinity. In the same vein w and z are input and output signal which quantified the robustness of the system

Hence,

The control input u is equivalent or directly proportional to the measured output y from the H infinity controller as:

$$u = Ky \quad (19)$$

The controller K for the optimal and multivariable performance of the inverter can be obtained from the closed loop transfer function of the system by adding equations (18) and (19) into Figure 1 and equation (20) was obtained.

$$z = \{P_{11}(s) + P_{12}(s)K[1 - P_{22}(s)K]^{-1}P_{21}(s)\}w \quad (20)$$

Where  $\|F_l(P, K)\|_\infty$  depicts the transformation of the plant (P) with controller K.

$$S(s) = (1 + G(s)K(s))^{-1} \quad (21)$$

$$T(s) = 1 - S(s) \quad (22)$$

Equation (21) shows how the output reject the disturbances from the input signal and equation (22) detail the tracking between the output and the input parameters.

## 2.3 Development of the PV System in SSA Tracker

The salp swarm biosphere of the random population is sectioned into: (i) leader at the front, and (ii) subsequent followers. The position of the salps is defined in an n-dimensional vector. Where n denotes the design variable numbers.

The population of salps X comprises of Number (N) agents with Dimension (D). Therefore, it can be defined by a  $N \times d$ -dimensional matrix in Equation (23)

$$X_1 = \begin{bmatrix} x_1^1 & x_1^2 & \dots & x_1^d \\ x_2^1 & x_2^2 & \dots & x_2^d \\ \vdots & \vdots & \ddots & \vdots \\ x_N^1 & x_N^2 & \dots & x_N^d \end{bmatrix} \quad (23)$$

## 2.4 Simulation Parameter

In this work, the parameters of a Shanghai Solar Energy S&T S-90C-1PV module and semi quasi inverter are simulated using MATLAB software by modelling the solar cell. The simulation is done on the datasheet of the Shanghai Solar Energy S&T S-90C-1 module. Table 1 shows solar module parameter. Hence the following expression is obtained from semi quasi inverter (SQSI) as also presented in Table 2

Table 1: PV module parameter (Deepamangai & Manoharan 2019)

Parameters	Values
Maximum Power ( $P_{max}$ )	90W
Current at $P_{max}$ ( $I_{mp}$ )	4.1A
Short-circuit current ( $I_{sc}$ )	4.9
Open-circuit voltage ( $V_{oc}$ )	26V
Voltage at $P_{max}$	22V

**Table 2: Simulation parameters for Semi Quasi Source Inverter (SQSI)**

Parameter	Value
Supply frequency	50Hz
SQSI Capacitance	4 $\mu$ F
SQSI inductance	400uH
Grid impedance	$l_g \in [0.1 \text{ to } 0.3] \text{ mH}$ and $r_g \in [0.001 \text{ to } 0.3] \Omega$
Grid voltage	230V
Switching frequency	40kHz

### 3.0 Results and Discussion

This section presents and discuss the analysis of the results of the developed scheme carried out in Matlab environment. The results obtained from the simulations were validated with robust controller for grid connected quasi admittance source inverter (QYSI) for PV system. Reinforcement language Algorithm was used for the maximum power point tracking (RLMPPT).

#### 3.1 PV Power and Conversion efficiency

The system simulation results of the power output (90W) is depicted in figure 2, the I-V and P-V curve characteristics of the PV system experience obvious changes due to variance in amount of solar irradiance striking the modules. A drastic increase in solar irradiance, there is a corresponding drastic increase in the photovoltaic current and slightly increase in the open circuit voltage (Voc). Consequently, the maximum available power also appreciate and vice versa.

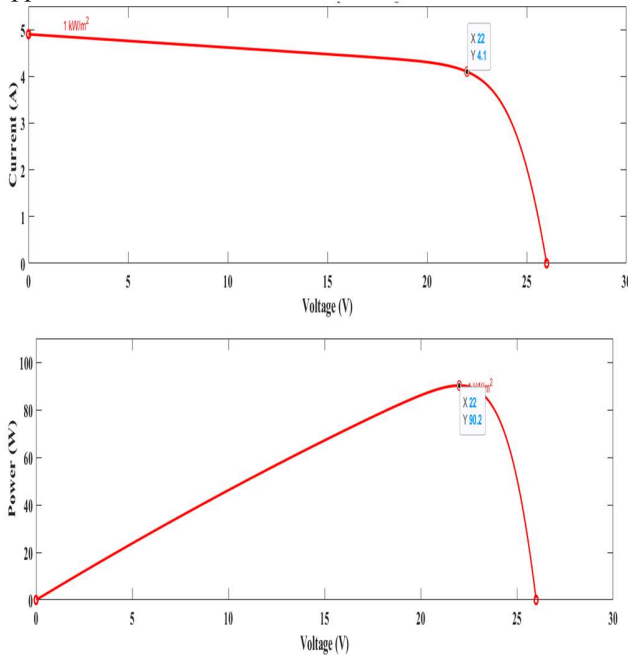


**Figure 2: I-V and P-V curves Characteristic**

#### 3.1.1 Semi Quasi Source Inverter (SQSI) with Salp Swarm Algorithm

The corresponding PV power of the system shown in Figure 3a, indicate constant condition and sudden changes in PV. The irradiance speed is adjusted from  $1000 \text{ ms}^{-2}$  to  $500 \text{ ms}^{-2}$  at 0.25s and it converged effectively. The output power from the solar inverter is 180W. It is obtained from two (2) number 90W solar panel connected in series, also observed that the SQSI approaches the steady state within the first period (20ms). The salp swarm algorithm track the maximum power point (MPP) adequately in conjunction with the controller mixed sensitivity function. Figure 3b shows the conversion efficiency using Salp Algorithm, it tracked the system more effectively and conversion efficiency improved from 97.1 to 99.68%.

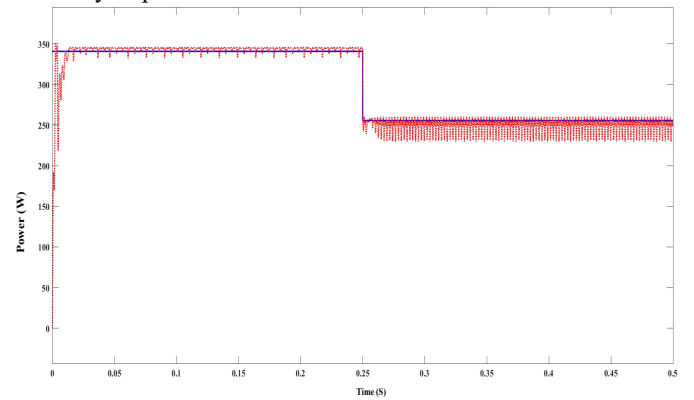


**Figure 3a: power output for SQSI using Salp Swarm Algorithm**

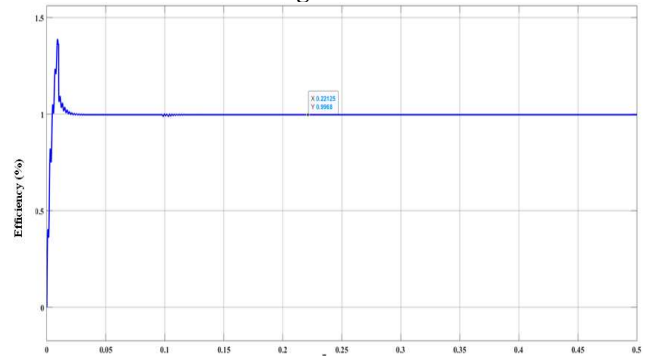


**Figure 3b: Conversion efficiency for SQSI using Salp Swarm Algorithm**

#### 3.1.2 Quasi Admittance Source Inverter with RLMPP Algorithm

The corresponding PV output of the system is shown in Figure 4. The RLMPPPT tracked the MPP efficiently, while the conversion efficiency is 97.1%. The insolation is varied from  $1000 \text{ ms}^{-2}$  to  $500 \text{ ms}^{-2}$  at 0.25s and it converged. However, the irradiance does not converge instantly it takes more than two period before reaching the steady state (that is beyond 0.04s).

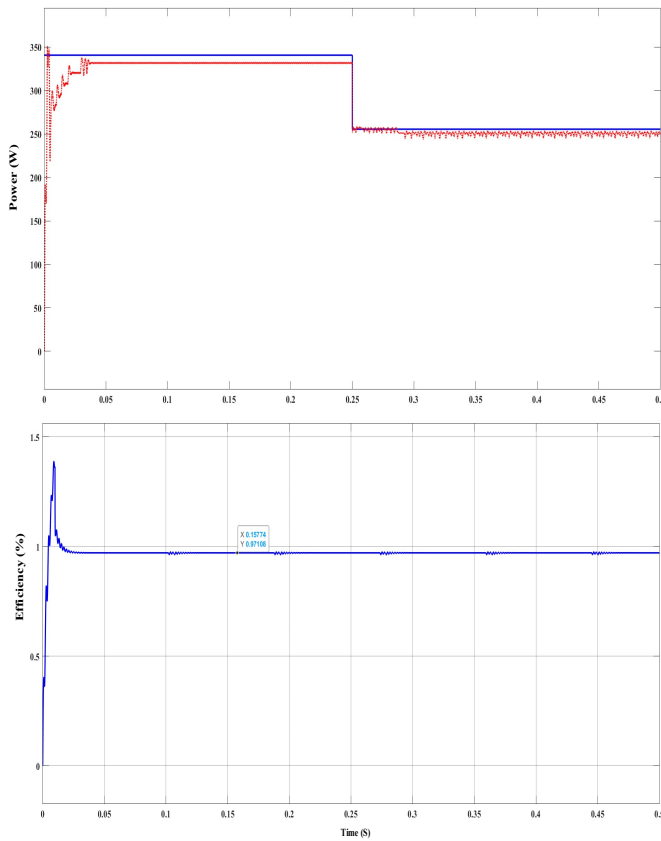


Figure 4: System output and efficiency for QYSI with RLMPT

### 3.2 Controller Performance

Three scenarios were used for showing the output of the controller based on stability gap and power quality improvement. These scenarios include: changes in grid impedance, frequency and harmonics. The simulation result was validated with robust controller for grid connected quasi admittance source inverter (QYSI) for PV system.

#### 3.2.1 Grid impedance variation for QYSI

The results of the system for the  $H_\infty$  controller with QYSI is as shown in Figure 5 (Deepamangai and manoharam, 2019). The high impedance resulted from the admittance of the quasi-source inverter, negatively affected the system stability and this is noticed on the grid current.

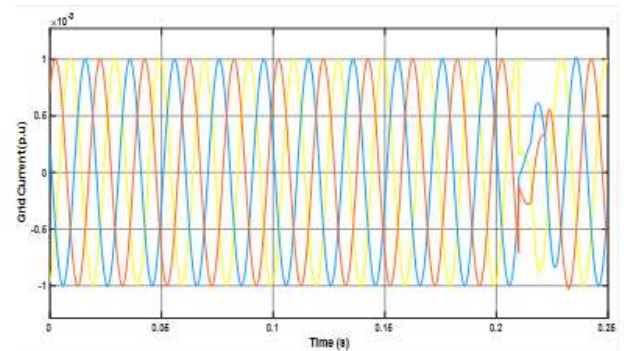
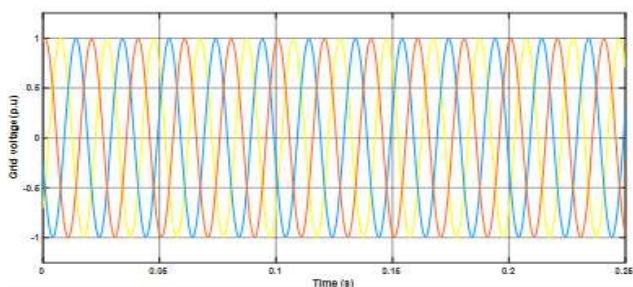


Figure 5: Grid inductance variation of  $H_\infty$  controller QYSI.

#### 3.2.2 Grid impedance variation for SQSI

Figure 6 shows result obtained when  $H_\infty$  controller was incorporated with the SQSI. Virtual impedance (grid inductance varying from 0.1mH to 0.3mH and grid resistance varying from 0.01ohm to 0.1ohm) was added to the system at  $t = 0.21s$ . The low level of the inductance in the inverter provides more stability in grid tied system.

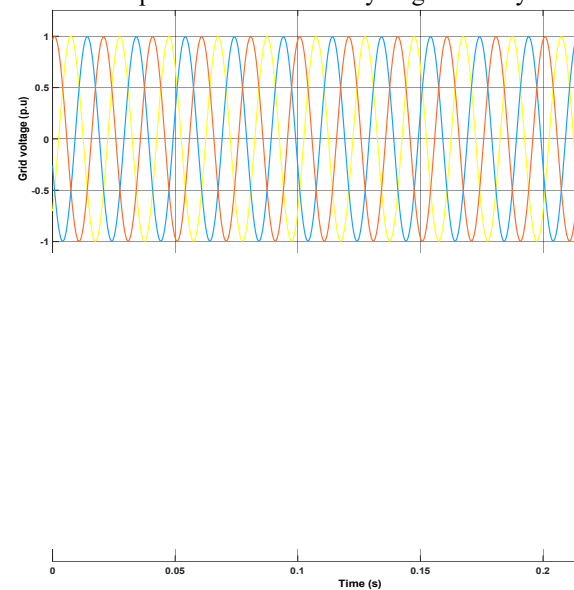
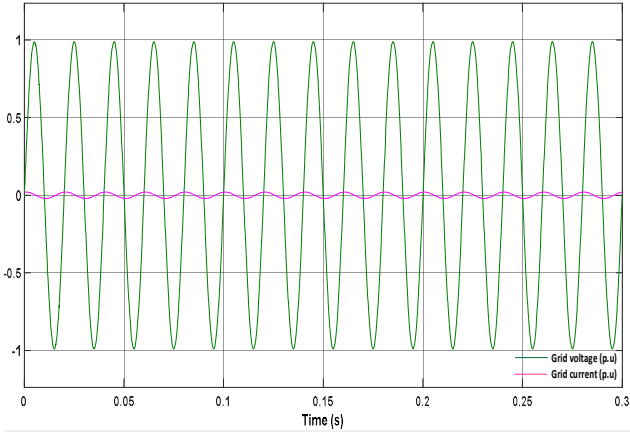


Figure 6: Grid inductance variation of  $H_\infty$  controller with SQSI.

#### 3.2.3 Grid frequency variation for QYSI

In this scenario, the frequency of the system is bounded with the range of  $\pm 1\%$ . Figure 7 depicts the grid tied current and voltage on frequency modification for the  $H_\infty$  controller with QYSI. It is observed that there is a phase differences between grid system current and voltage. Hence, the power factor was 0.90.



**Figure 7: Variation on frequency from 50 Hz to 50.3 Hz: Grid-tied voltage and current for H $\infty$  controller with QSI**

**3.3.4 Grid frequency variation for SQSI**

At first, the grid system voltage per phase was placed at 230 V, and 50 Hz. At time  $t = 0.21s$ , the system grid is still bounded with the range of plusof $\pm 1\%$ . The addition of virtual load at  $t = 0.21s$ , the SQSI frequency been altered to 50.30 Hz, and restored to 50 Hz at 0.25s when removed. Figure 8 depicts the grid power quality behavior regarding to the voltage and current when varying the frequency for the H $\infty$  system controller with SQSI. The applied method tracks the frequency fluctuation with a minimal error. A phase lag between grid system current and voltage with a power factor of 0.96. Hence, the H $\infty$  controller with SQSI provides better outputs as compared to robust controller for grid connected quasi admittance source inverter (QYSI) for PV system.

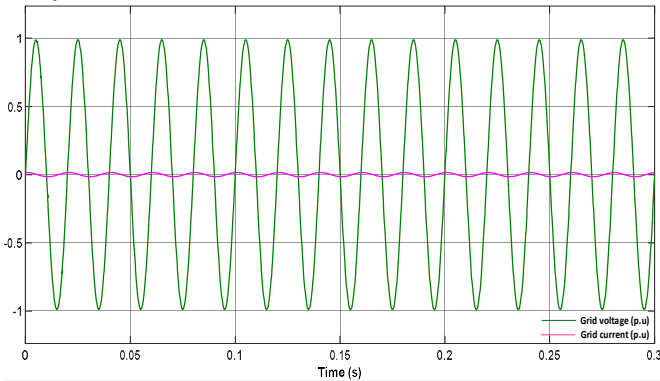


**Figure 8: Variation on frequency from 50 Hz to 50.3 Hz: Grid-tied voltage and current for H $\infty$  controller with SQSI**

**3.3.5 Grid harmonics distortion**

The Analysis showed that the distorted source current waveform contains high level of harmonics and has a Total Harmonic Distortion (THD). The disturbance (THD) on the system grid is depicted in Figure 9a for varying grid inductance, the grid-tied voltage and current have THD of 0.61% with SQSI. There is obvious improvement using the

same controller (H infinity) with SQSI when compared with robust controller for grid connected quasi admittance source inverter (QYSI) for PV the inverter has a THD of 0.67% as shown in Figure 9b. It is obviously showed that the H $\infty$  controller sustain the system reliability despite the disturbances of grid impedances in conjunction with SQSI.

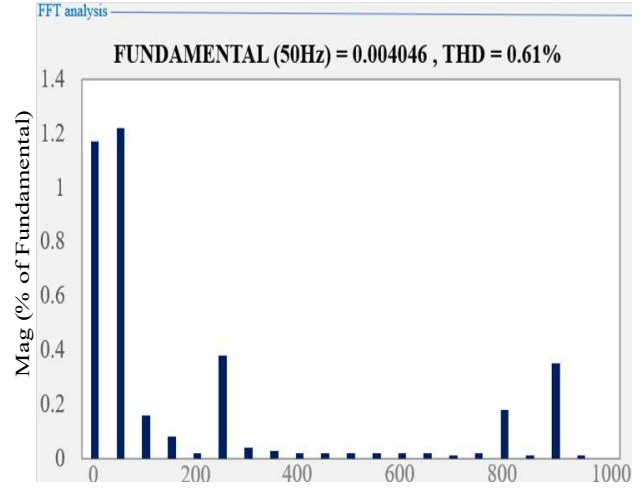


**Figure 9a: Grid current harmonics for H $\infty$  Controller with SQSI**

FFT analysis revealed that the distorted current waveform contains harmonics and has a THD value of 0.67%, which was observed to be much higher compare with the value obtained with SQSI.

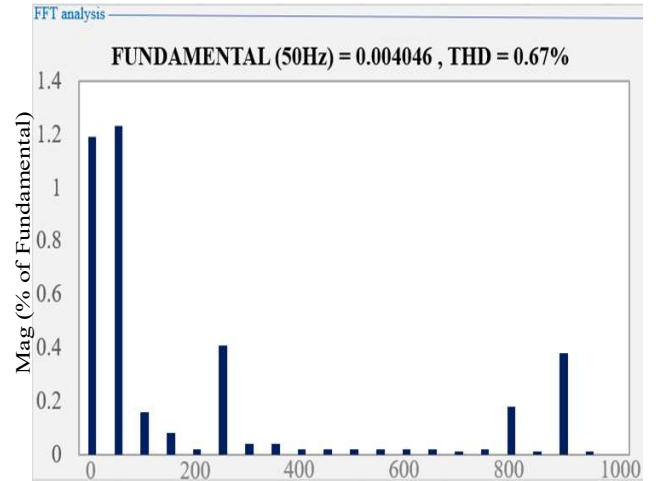


**Figure 9b: Grid current harmonics for H $\infty$  Controller with QYSI**

Table 2 shows the summary of results obtained regarding to the tracking efficiency of the proposed method while Table 3 shows the summary of THD result obtained.

**Table 2: Summary of Results of Tracking Efficiency**

	Efficiency Comparison
Deepamangai and Manoharan (2019)	97.11%
Proposed method	99.68%
Percentage improvement	2.6%

**Table 3: THD Comparison**

	THD Comparison
Deepamangai and Manoharan (2019)	0.67%
Proposed method	0.61%
Percentage improvement	8.95%

#### 4.0 Conclusion

This research work presents the implementation of  $H_{\infty}$  (H infinity) system for a grid-tied SQSI for adequate system reliability and better power quality improvement. The SQSI reduces the voltage stress on the component, start-up inrush current, and also increases the modulation index. The  $H_{\infty}$  controller provide adequate power stability for the SQSI system under the grid-tied load variations. The robustness analysis of the system satisfied and guaranteed controller system. The distortions of current wave form on SQSI has also been compared and the results affirmed the improvement of the proposed technique with low level of Total Harmonics Distortion (THD). The Fast Fourier Transform (FFT) analysis showed that the THD was reduced from 0.67% to 0.61% by the application of semi quasi source inverter (SQSI) and also the phase angle has been improved in terms of power factor for power quality improvement. The salp swarm algorithm track the irradiance effectively with improve value from 97.11% to 99.68% for maximum collections of current from the solar modules, when compared with robust controller for grid connected quasi admittance source inverter (QYSI) for PV system.

#### References

Abdelrahem, M., Ismeil, M. A., Orabi, M., & Kennel, R. (2019). *Three phase Semi-Z-Source Inverter for PV Applications*. Paper presented at the PCIM Europe 2019; International Exhibition and Conference for Power Electronics, Intelligent Motion, Renewable Energy and Energy Management 1-6.

Abdulwahab, I., Abubakar, A. S., Olaniyan, A., Sadiq, B. O., & Faskari, S. A. (2022). *Control of Dual Stator Induction Generator Based Wind Energy Conversion System*. Paper presented at the 2022 IEEE Nigeria 4th International Conference on Disruptive Technologies for Sustainable Development (NIGERCON) 1-5.

Babaita, A., Mati, A., Jibril, Y., Kunya, A., & Abdulwahab, L. (2022). *DEVELOPMENT OF A LOAD FREQUENCY CONTROL SCHEME FOR AN AUTONOMOUS HYBRID MICROGRID*. *Zaria Journal of Electrical Engineering Technology*, 11(1).

Deepamangai, P., & Manoharan, P. (2019). Robust controller for grid-connected quasi-admittance source inverter for photovoltaic system. *Electric Power Systems Research*, 175, 105879.

Fang, X., Ma, B., Gao, G., & Gao, L. (2018). Three phase trans-Quasi-Z-source inverter. *CPSS Transactions on Power Electronics and Applications*, 3(3), 223-231.

Hassan, T. K. (2017). APPLICATION OF QUASI-Z-SOURCE INVERTER IN PHOTOVOLTAIC GRID-CONNECTED SYSTEMS. *Journal of Engineering and Sustainable Development*, 21(02).

Iliyasu, M. U., Ozohu, M., Yusuf, S. S., Abdulwahab, I., Ehime, A., & Umar, A. (2022). Development of an Optimal Coordination Scheme For Dual Relay Setting In Distribution Network Using Smell Agent Optimization Algorithm. *COVENANT JOURNAL OF ENGINEERING TECHNOLOGY*.

Ismeil, M. A., Orabi, M., & Ahmed, M. (2018). *Single-phase cascaded semi-Z-source inverter for photovoltaic applications*. Paper presented at the 2018 International Conference on Innovative Trends in Computer Engineering (ITCE) 398-402.

Rasool, M. A. U., Khan, M. M., Ahmed, Z., & Saeed, M. A. (2019). Analysis of an  $h_{\infty}$  robust control for a three-phase voltage source inverter. *Inventions*, 4(1), 18.

Santhoshi, K. B., Mohana Sundaram, K., Padmanaban, S., Holm-Nielsen, J. B., & KK, P. (2019). Critical review of PV grid-tied inverters. *Energies*, 12(10), 1921.

Venkatesan, M., Balachander, K., & Kumar, S. R. (2019). PWM Controlled 3-Phase Inverter for Renewable Energy Applications and Environmental Impacts. *Journal of Green Engineering (JGE)*, 9(2), 189-200.